

# We are IntechOpen, the world's leading publisher of Open Access books Built by scientists, for scientists

**4,800**

Open access books available

**122,000**

International authors and editors

**135M**

Downloads

Our authors are among the

**154**

Countries delivered to

**TOP 1%**

most cited scientists

**12.2%**

Contributors from top 500 universities



**WEB OF SCIENCE™**

Selection of our books indexed in the Book Citation Index  
in Web of Science™ Core Collection (BKCI)

Interested in publishing with us?  
Contact [book.department@intechopen.com](mailto:book.department@intechopen.com)

Numbers displayed above are based on latest data collected.

For more information visit [www.intechopen.com](http://www.intechopen.com)



# Crystallographic Studies on Autophagy-Related Proteins

Nobuo N. Noda<sup>1</sup>, Yoshinori Ohsumi<sup>2</sup> and Fuyuhiko Inagaki<sup>3</sup>

<sup>1</sup>*Institute of Microbial Chemistry, Tokyo*

<sup>2</sup>*Tokyo Institute of Technology*

<sup>3</sup>*Hokkaido University*

*Japan*

## 1. Introduction

Autophagy is an intracellular bulk degradation system conserved in most eukaryotes. Autophagy plays various physiological roles such as intracellular clearance, development, differentiation and intracellular immunity, and its dysfunction is related to severe diseases such as neurodegeneration and cancer (Mizushima, 2007; Mizushima et al., 2008). Upon induction of autophagy, isolation membranes appear in the cytoplasm and expand to enclose a portion of the cytoplasm to be double membrane structures, autophagosomes (Mizushima et al., 2011; Nakatogawa et al., 2009). In some cases, organelles such as mitochondria and peroxisomes, and even invading microbes are also enclosed. All the matters enclosed by an autophagosome are named cargoes. The autophagosome fuses with the lysosome in mammals and with the vacuole in yeast and plants and exposes its inner membrane containing cargoes to vacuolar/lysosomal hydrolases, which degrade cargoes. Using the budding yeast, *Saccharomyces cerevisiae*, as a model organism, many ATG genes required for autophagy, especially in the step of autophagosome formation, have been identified (Klionsky et al., 2003; Tsukada and Ohsumi, 1993). Most ATG genes are evolutionarily conserved among higher eukaryotes including mammals, suggesting that the basic molecular mechanisms of autophagy are also evolutionarily conserved. Of the 35 Atg proteins identified thus far, 18 have been shown as crucial for autophagosome formation (Nakatogawa et al., 2009). However, it remains to be elucidated how these Atg proteins mediate autophagosome formation. In order to establish the molecular functions of each Atg protein and unveil the mechanism of autophagy, we started comprehensive structural studies of Atg proteins using X-ray crystallography. In this chapter, we review X-ray crystallographic studies of Atg proteins focusing on experimental details. For a more detailed description of the structure and function of Atg proteins, please refer to other recent reviews (Mizushima et al., 2011; Nakatogawa et al., 2009; Noda et al., 2009, 2010).

## 2. X-ray crystallographic studies of Atg proteins involved in ubiquitin-like conjugation reactions

Of the 18 Atg proteins essential for autophagosome formation, eight, namely, Atg3, Atg4, Atg5, Atg7, Atg8, Atg10, Atg12 and Atg16, constitute two ubiquitin-like conjugation

systems: the Atg8 system and the Atg12 system (Nakatogawa et al., 2009) (Figure 1). In the Atg8 system, the ubiquitin-like protein Atg8 is first processed by the cysteine protease Atg4 (Kirisako et al., 2000). The exposed C-terminal Gly116 of Atg8 is activated by Atg7, an E1-like enzyme, to form an Atg7~Atg8 thioester intermediate (Tanida et al., 1999). Then, Atg8 is transferred to Atg3, an E2-like enzyme, to form an Atg3~Atg8 thioester intermediate (Ichimura et al., 2000). Finally, Gly116 of Atg8 is conjugated to a phosphatidylethanolamine (PE) to form Atg8–PE conjugates (Ichimura et al., 2000), in which Atg12–Atg5 conjugates (mentioned below) play crucial roles (Fujioka et al., 2008a; Hanada et al., 2007). Atg8–PE conjugates localize to isolation membranes and autophagosomes (Kirisako et al., 1999) and play crucial roles in both autophagosome formation and cargo recognition during autophagy. In the Atg12 system, the C-terminal Gly186 of another ubiquitin-like protein, Atg12, is activated by Atg7 to form an Atg7~Atg12 thioester intermediate. Then, Atg12 is transferred to Atg10, an E2-like enzyme, to form an Atg10~Atg12 thioester intermediate (Shintani et al., 1999). Finally, Gly186 of Atg12 is conjugated to the lysine side chain of Atg5 to form Atg12–Atg5 conjugates (Mizushima et al., 1998). Atg12–Atg5 conjugates form a complex with Atg16 through the direct interaction between Atg5 and Atg16 and localize to isolation membranes in the form of the Atg12–Atg5–Atg16 ternary complex (Mizushima et al., 2003; Mizushima et al., 1999). The Atg12–Atg5–Atg16 ternary complex also plays crucial roles in autophagy, one of which is an E3-like function in the Atg8 system.

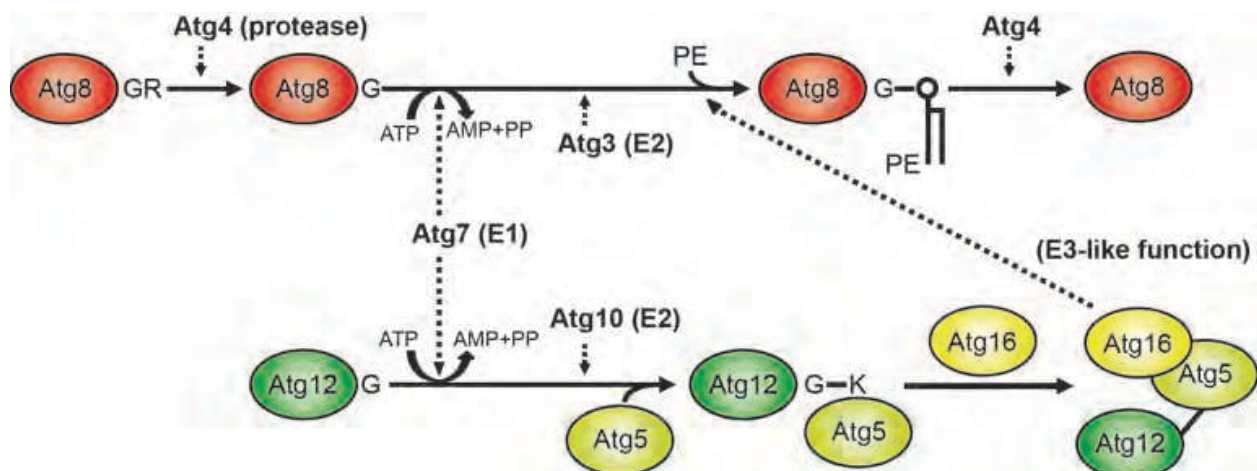


Fig. 1. Atg conjugation systems. Atg12 is irreversibly conjugated to Atg5 by Atg7 and Atg10, and the Atg12–Atg5 conjugate further forms a complex with Atg16. Atg8 is reversibly conjugated to PE by Atg3, Atg4, Atg7 and Atg12–Atg5–Atg16 complex.

The molecular mechanism of conjugation reactions in the Atg8 and Atg12 systems has been considered similar to that of ubiquitylation. However, all Atg proteins involved in such reactions have a low sequence homology with proteins involved in ubiquitylation and other ubiquitin-like modification systems. Moreover, the Atg8 system mediates a unique protein-lipid conjugation reaction, whereas the Atg12 system mediates the modification of only a single target protein. Owing to these unique features of the Atg conjugation systems, it is difficult to speculate the precise molecular mechanisms of the above conjugation reactions on the basis of our knowledge of other modification systems. In addition to the conjugation reaction mechanism, the molecular roles of Atg8–PE and Atg12–Atg5–Atg16 complex in autophagy also present critical problems that require elucidation. In order to answer these

problems, we started comprehensive structural studies of Atg proteins involved in the Atg8 and Atg12 systems using mainly X-ray crystallography.

## 2.1 Atg8-family proteins

Atg8 is a ubiquitin-like modifier involved in autophagy, and is conjugated to the amino group of PE through ubiquitin-like reactions as mentioned above. Atg8–PE conjugates localize to autophagic membranes, and play at least two critical roles in autophagy: one is autophagosome formation (Nakatogawa et al., 2007), and the other is selective cargo recognition (Noda et al., 2008b). Atg8 was the first Atg protein we attempted to crystallize; however, we could not obtain any crystals for Atg8. At that time, LC3 was identified as a mammalian Atg8 ortholog and was shown to play crucial roles in mammalian autophagy. Therefore, we switched the crystallization target from Atg8 to LC3 and performed an X-ray crystallographic study of LC3 at first. Much later, we succeeded in obtaining crystals of Atg8 and determined the crystal structure of Atg8.

### 2.1.1 LC3

Microtubule-associated protein light chain 3 (LC3) is a mammalian ortholog of Atg8 and is conjugated to PE through ubiquitin-like reactions similarly to Atg8 (Kabeya et al., 2000). Since LC3–PE localizes to isolation membranes and autophagosomes, it is widely used as a marker protein for autophagic membranes (Kabeya et al., 2000; Mizushima et al., 2010). Rat LC3 is composed of 142 amino acids. The C-terminal 22 residues (121–142), which are processed by a mammalian Atg4 homolog (Atg4B) (Kabeya et al., 2004), are not important for the function of LC3. Thus, we performed a structural study of the processed form of LC3 (residues 1–120). LC3 was well expressed in *E. coli* as a soluble protein, and was easily crystallized into forms I and II crystals (Sugawara et al., 2003). Although the form I crystal diffracted poorly ( $\sim 3.5$  Å), the form II crystal diffracted up to 2.05 Å resolution. Thus, using the form II crystal, we determined the crystal structure of LC3 by the molecular replacement method (Sugawara et al., 2004). As a search model, the crystal structure of GATE-16, another mammalian homolog of Atg8, was used. As shown in Figure 2A, the presence of two  $\alpha$ -helices ( $\alpha 1$  and  $\alpha 2$ ) at the N-terminal side of the ubiquitin fold is a structural feature of LC3 and all Atg8-family members (Noda et al., 2009, 2010).

### 2.1.2 Atg8

Atg8 is composed of 117 amino acids, and immediately after translation, it is processed by Atg4 to expose Gly116 at the C-terminus. The processed form of Atg8 (1–116) was well expressed in *E. coli* as a soluble protein and highly purified; however, it was never crystallized. An NMR study of Atg8 suggested that the N-terminal region of Atg8, which corresponds to  $\alpha 1$  and  $\alpha 2$  of LC3, does not have a rigid uniform conformation (Kumeta et al., 2010), which was suggested to hamper the crystallization of Atg8. Although we could not crystallize Atg8 alone, we succeeded in obtaining good crystals of Atg8 as a complex with its binding peptide. The used 4-residue peptide, Trp-Glu-Glu-Leu, corresponds to the C-terminal four residues of Atg19, an autophagic receptor protein involved in the selective transport of vacuolar enzymes into the vacuole through autophagic processes (Scott et al., 2001). Thus we determined the crystal structure of Atg8 as a complex with a peptide by the molecular replacement method (Noda et al., 2008b). As shown in Figure 2B, the peptide has an extended conformation and forms an intermolecular  $\beta$ -sheet with  $\beta 2$  of Atg8.

Furthermore, the hydrophobic side-chains of Trp and Leu of the peptide bind to the two hydrophobic pockets, namely, the W-site and L-site, respectively, and the acidic side-chains of two Glu residues of the peptide form ionic interaction with basic Arg28 and Arg67 of Atg8. These interactions significantly stabilize the conformations of  $\alpha 1$  and  $\alpha 2$  of Atg8, and thus promote the crystallization of Atg8.

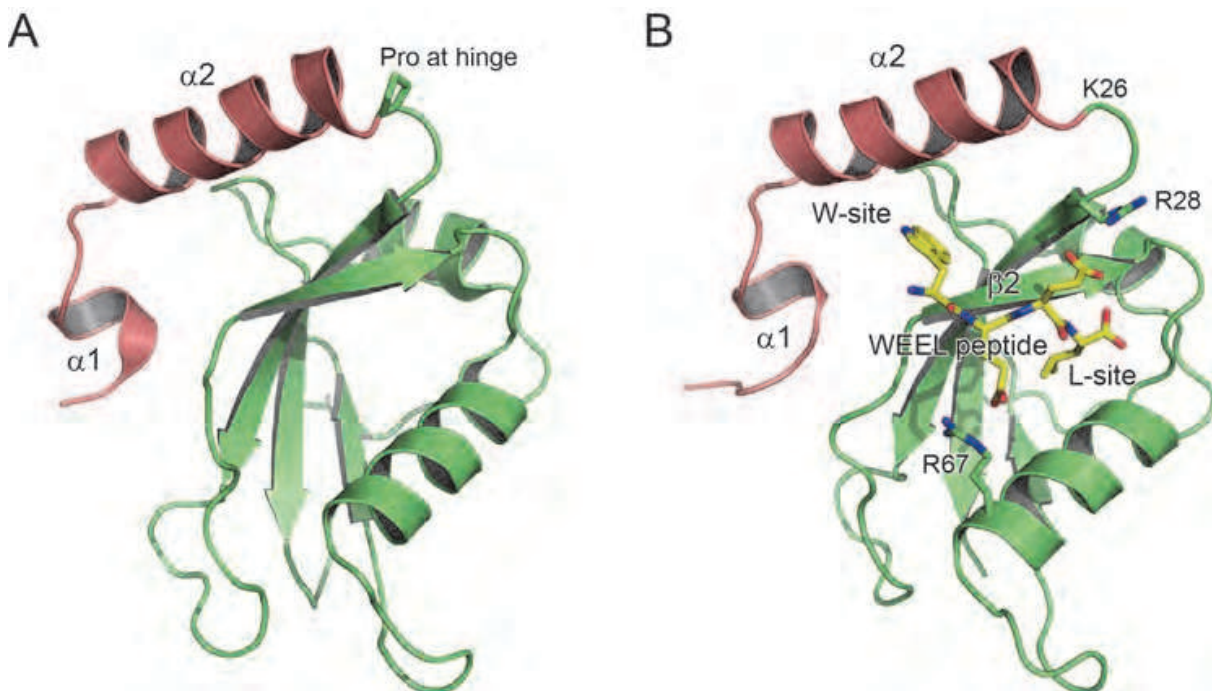


Fig. 2. Structure of LC3 (left) and Atg8 in complex with a WEEL peptide (right). The N-terminal region unique to Atg8-family proteins are colored salmon pink.

In contrast to ligand-free Atg8, which is difficult to crystallize, three mammalian Atg8 homologs (i.e., LC3, GATE-16 and GABARAP) are easily crystallized in free form. We noticed that in the hinge region between  $\alpha 2$  and the ubiquitin fold moiety, a Pro residue is conserved among mammalian Atg8 homologs but not in Atg8. We thought that the introduction of a Pro residue into the hinge will stabilize the N-terminal region of Atg8. As expected, the substitution of Lys26 with Pro increased the stability of Atg8 and significantly improved the NMR spectra obtained from the mutant protein. Using this mutant, we determined the solution structure of Atg8 by NMR, showing that the N-terminal region of Atg8 has a convergent conformation similar to that of mammalian Atg8 homologs (Kumeta et al., 2010). This mutation affected neither the conjugation of Atg8 with PE nor the autophagic activity in yeast cells (Kumeta et al., 2010), suggesting that the flexible nature of the N-terminal region of Atg8 is not important for the function of Atg8 and that Atg8 K26P can be used for structural study as a fully active protein. We actually used this mutant for analyzing the interaction between Atg8 and Atg3 with NMR spectroscopy (Yamaguchi et al., 2010).

## 2.2 Atg12

Atg12 is another ubiquitin-like modifier involved in autophagy and is conjugated to the lysine side chain of Atg5 through ubiquitin-like reactions. Atg12 has several unique features

compared with other ubiquitin-like modifiers. First, *S. cerevisiae* Atg12 is composed of 186 amino acids and is much larger than ubiquitin and other ubiquitin-like proteins including Atg8. Second, no processing/deconjugating enzyme for Atg12 has been reported, and thus its conjugation reaction appears to be irreversible. Third, the modification target for Atg12 is restricted to a single protein, Atg5 (although Atg3 was reported to be another modification target for Atg12 in mammals (Radoshevich et al., 2010)). Finally, Atg12 has little sequence homology with other ubiquitin-like proteins. To establish the structure and function of Atg12, we started its structural study.

Unlike ubiquitin and other ubiquitin-like modifiers, soluble recombinant Atg12 could not be obtained from *E. coli*. We also tried to prepare recombinant proteins for a mammalian Atg12 homolog but failed for the same reason as above. We then performed multiple sequence alignment among Atg12 homologs and noticed that the *Arabidopsis thaliana* Atg12 homologs AtAtg12a and AtAtg12b are composed of only 96 and 94 amino acids, respectively, and thus are much smaller than other Atg12 homologs. The smaller size of AtAtg12s seemed advantageous for the preparation of recombinant proteins and crystallization, so we switched the crystallization target from Atg12 to AtAtg12s.

Although every component of the Atg12 system has already been found in the *Arabidopsis* genome at that time, it remains to be shown that they are functional orthologs of yeast ATG genes and crucial for plant autophagy. Thus, before our structural study, we performed functional analyses of AtAtg12a and AtAtg12b (Suzuki et al., 2005). We first attempted to detect AtAtg12-AtAtg5 conjugates in *Arabidopsis* using antibodies against AtAtg12s. We detected AtAtg12-AtAtg5 conjugates in wild-type plants. In contrast, we could not detect them in *Atatg5-1/Atatg5-1* and *Atatg10-1/Atatg10-1* plants. Consistently, *Atatg5-1/Atatg5-1* or *Atatg10-1/Atatg10-1* plants showed no autophagic activity. Taken together, these data suggest that the Atg12 system is also conserved in *Arabidopsis* and plays an essential role in plant autophagy.

We then started structural studies of AtAtg12s. Although AtAtg12a and AtAtg12b have a similar size (96 versus 94 amino acids) and high sequence identity (93%), only AtAtg12b was obtained from *E. coli* as a soluble protein. During purification, AtAtg12b behaved as both a monomer and a dimer, and an irreversible change from a monomer into a dimer was observed during purification. The dimeric form of AtAtg12b showed higher solubility and stability than the monomeric form, and only the dimeric form crystallized. The obtained crystals diffracted up to 1.8 Å resolution, and the crystal structure of AtAtg12b was determined by the multiple isomorphous replacement method (MIR) (Suzuki et al., 2005).

Surprisingly, AtAtg12b existed as an intertwined dimer in the crystal (Figure 3). The loop connecting residues 58 and 61 acted as a hinge for domain swapping, and the 61-94 region was exchanged between the two molecules. In spite of domain swapping, the split half of the hinge has a canonical ubiquitin fold. The intertwined dimer structure in the crystal presumably represents the dimer structure in solution; however, dimer formation itself appears to be an *in vitro* artifact. *In vivo*, most Atg12 exists as a conjugate with Atg5, and in the absence of Atg16, Atg12-Atg5 conjugates exist as a monomer (Kuma et al., 2002). We also prepared recombinant proteins for Atg12-Atg5 conjugates (Noda et al., 2008a), which existed as a monomer in solution. These observations suggest that free Atg12 is unstable and significantly stabilized by conjugation with Atg5 both *in vitro* and *in vivo*. On the other hand, AtAtg12b appears to be artificially stabilized by domain swapping *in vitro*. The unstable

nature of Atg12, which is unique compared with ubiquitin and other ubiquitin-like proteins, might hold the key to Atg12-specific functions.

The monomeric structure of AtAtg12b (the split half of the intertwined dimer) consists of an ubiquitin fold and has no unique insertions. However, the ubiquitin fold has a hydrophobic patch that is conserved among Atg12 homologs but not among other ubiquitin-like modifiers (Suzuki et al., 2005). Mutation at this patch of yeast Atg12 causes a severe defect in autophagy (Hanada and Ohsumi, 2005), suggesting that the conserved patch is crucial for the Atg12 function in autophagy.

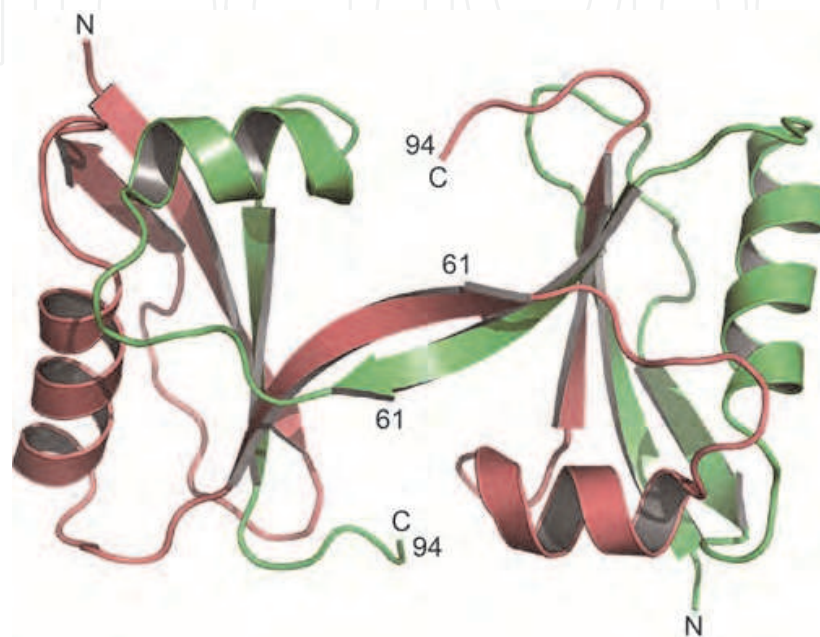


Fig. 3. Crystal structure of the intertwined dimer of AtAtg12b. Two polypeptides are colored green and salmon pink, respectively. N- and C-termini are labeled N and C, respectively.

### 2.3 Atg3

Atg3 is an E2-like enzyme in the Atg8 system. Atg3 receives Atg8 from an Atg7~Atg8 thioester intermediate to form an Atg3~Atg8 thioester intermediate. Then, with the help of the Atg12—Atg5-Atg16 complex (see below), Atg3 transfers Atg8 to PE. Atg3 is unique among E2-family proteins in that it mediates the conjugation reaction between a protein and a lipid. Atg3 has a low sequence homology with canonical E2 enzymes, and at 36 kDa is larger than them (typically around 20 kDa). Owing to these unique features of Atg3, it was difficult to speculate about the structure of Atg3 without experimental information.

Atg3 is composed of 310 amino acids. Full-length Atg3 was expressed as a GST-fusion protein in *E. coli*, in which two plasmids, pGEX-4T and pGEX-6P (GE Healthcare), were used. From the pGEX-4T and pGEX-6P vectors, GST-fused Atg3 with a thrombin and a PreScission protease-cleavage sequence, respectively, between GST and Atg3 were expressed. After affinity chromatography, GST was cleaved from GST-Atg3 using either thrombin or PreScission protease, resulting in Atg3 with a Gly-Ser (thrombin digestion) or Gly-Pro-Leu-Gly-Ser (PreScission digestion) artificial sequence at the N-terminus. These two Atg3s were subjected to crystallization screening. Intriguingly, crystals were obtained from Atg3 with a Gly-Ser artificial sequence, but not from Atg3 with a Gly-Pro-Leu-Gly-Ser

artificial sequence (Yamada et al., 2006). Thus, we used pGEX-4T-Atg3 for further studies, despite the fact that we usually use the pGEX-6P vector rather than the pGEX-4T vector since a PreScission protease has a higher activity than a thrombin protease at low temperature.

Using the obtained crystals, the crystal structure of Atg3 was determined by MIR (Yamada et al., 2007). Figure 4 shows the overall structure of Atg3. Atg3 has a unique hammer like shape consisting of a head and a handle. The head moiety has a topology similar to that of canonical E2 enzymes, whereas the handle region (HR) is unique to Atg3. In addition to HR, Atg3 has another large, unique insertion (~80 amino acids) in its head moiety. Most of the residues constituting this region were not modelled owing to a low electron density; thus, this region was named the flexible region (FR). NMR studies showed that Atg3 FR actually has a flexible conformation in solution (Yamada et al., 2007). Truncational studies showed that HR and FR are responsible for the interaction with Atg8 and Atg7, respectively, and play crucial roles in Atg8–PE formation (Yamada et al., 2007).

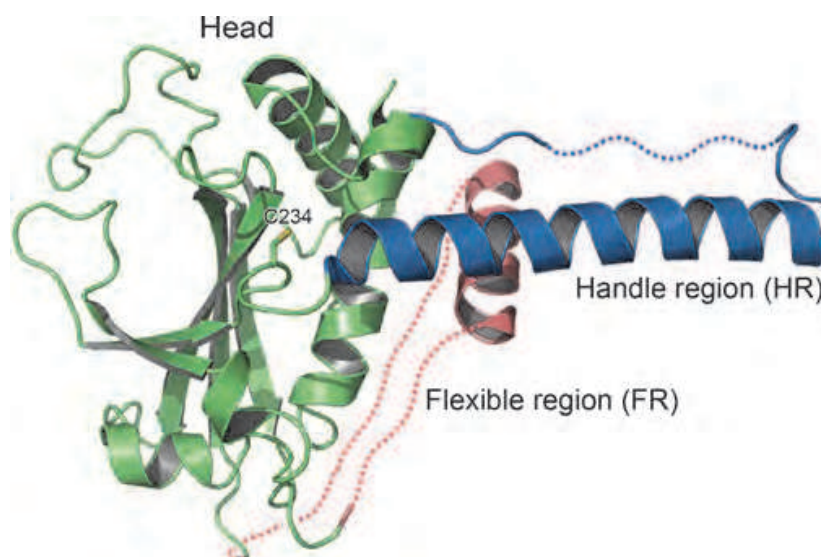


Fig. 4. Structure of Atg3. Head, FR and HR of Atg3 are colored green, salmon pink and blue, respectively. Disordered region in FR and HR is indicated as a broken line.

## 2.4 Atg4

Atg4 is the sole protease among all Atg proteins and mediates both the processing of the precursor Atg8 and the deconjugation of Atg8–PE. The reversible modification of Atg8 with PE is crucial for autophagy; therefore, Atg4 can be a target for developing autophagy-specific inhibitors. Although Atg4 was predicted to be a cysteine protease, it has little sequence homology with any known cysteine proteases. Thus, structural information on Atg4 was strongly desired for designing the specific inhibitors of this protein.

### 2.4.1 HsAtg4B as a free form

We first attempted to crystallize *S. cerevisiae* Atg4. However, we never obtained its crystals. Humans have four Atg4 homologs (4A–4D), among which Atg4B was reported to be responsible for LC3 processing and delipidation (Kabeya et al., 2004). Therefore, we changed the crystallization target from yeast Atg4 to human Atg4B (HsAtg4B). Full-length



HsAtg4B, which consists of 393 amino acids, crystallized easily, and the obtained crystals diffracted beyond 2 Å. The crystal structure of HsAtg4B was determined by the multi-wavelength anomalous dispersion method (MAD) using selenomethionine-substituted crystals (Figure 5A) (Sugawara et al., 2005).

The overall structure of HsAtg4B is composed of a papain-like fold conserved among cysteine proteases and a unique region that we named “the short Fingers domain” since its insertion site is similar to the “Fingers domain” of the herpesvirus-associated ubiquitin-specific protease, a cysteine protease structurally similar to HsAtg4B. Cys74 (catalytic cysteine), Asp278 and His280 form a catalytic triad in the crystal. The primary sequence order (Cys-Asp-His) of the catalytic triad is distinct from that of most cysteine proteases (Cys-His-Asp). Cys74 is buried under a loop named the regulatory loop and Trp142, suggesting that free HsAtg4B is autoinhibited. Consistent with the autoinhibited structure, a peptide corresponding to residues 116-124 of LC3, which include a scissile site of HsAtg4B (Gly120), was not processed by HsAtg4B (Sugawara et al., 2005). It was therefore proposed that in order to access the catalytic site of HsAtg4B and to be processed, the substrate (LC3) should induce a conformational change of HsAtg4B to release the autoinhibited structure.

#### 2.4.2 HsAtg4B-LC3 complex

We next attempted to determine the structure of HsAtg4B in complex with LC3. First, we crystallized full-length HsAtg4B in complex with LC3, but obtained no crystal. In the free HsAtg4B structure, the C-terminal 39 residues (residues 355-393) showed a low electron density, suggesting that they are highly flexible. Therefore, we used a truncated form of HsAtg4B (1-354) for co-crystallization with LC3, and obtained good crystals of the HsAtg4B(1-354)-LC3(1-120) complex (Satoo et al., 2007). Furthermore, we obtained two types of the HsAtg4B-LC3 precursor complex: HsAtg4B(1-354, H280A)-LC3(1-124) and HsAtg4B(1-354, C74S)-LC3(1-124) complexes. H280A and C74S mutations were introduced to prevent the cleavage of the LC3 precursor. Using these crystals, we determined three complex structures by the molecular replacement method (Satoo et al., 2009).

Figure 5B shows the structure of the HsAtg4B(1-354, C74S)-LC3(1-124) complex. A structural comparison between the free and complex structures suggests that LC3 induces a large conformational change in two regions in HsAtg4B: one is the regulatory loop and the other is the N-terminal tail. The regulatory loop and Trp142, which block the catalytic site of the free HsAtg4B structure, are lifted up by LC3 Phe119, forming a narrow groove under the loop, through which LC3 Gly120 has access to Cys74 of HsAtg4B. This structure explains why the Phe-Gly sequence of LC3 is essential for the hydrolysis by HsAtg4B. In addition to the C-terminal tail, the ubiquitin-fold core of LC3 also interacts with HsAtg4B, which may also be required for releasing the autoinhibited conformation of HsAtg4B. On the other hand, the N-terminal tail, which interacts with the papain-fold moiety of free HsAtg4B, is bound to the crystallographically adjacent LC3 molecule in the complex structure using a Tyr-X-X-Leu sequence. This conformational change exposes a large flat surface at the exit of the catalytic site. It is unclear whether this interaction is a crystallization artifact or whether it actually occurs in solution. Therefore, we performed NMR analysis, which clearly showed that the interaction observed in the crystal actually occurs in solution (Satoo et al., 2009). Although the biological significance of this interaction has not been proved yet, we propose

that the conformational change of the N-terminal tail of HsAtg4B regulates the accessibility of HsAtg4B to the membrane where LC3–PE is embedded.

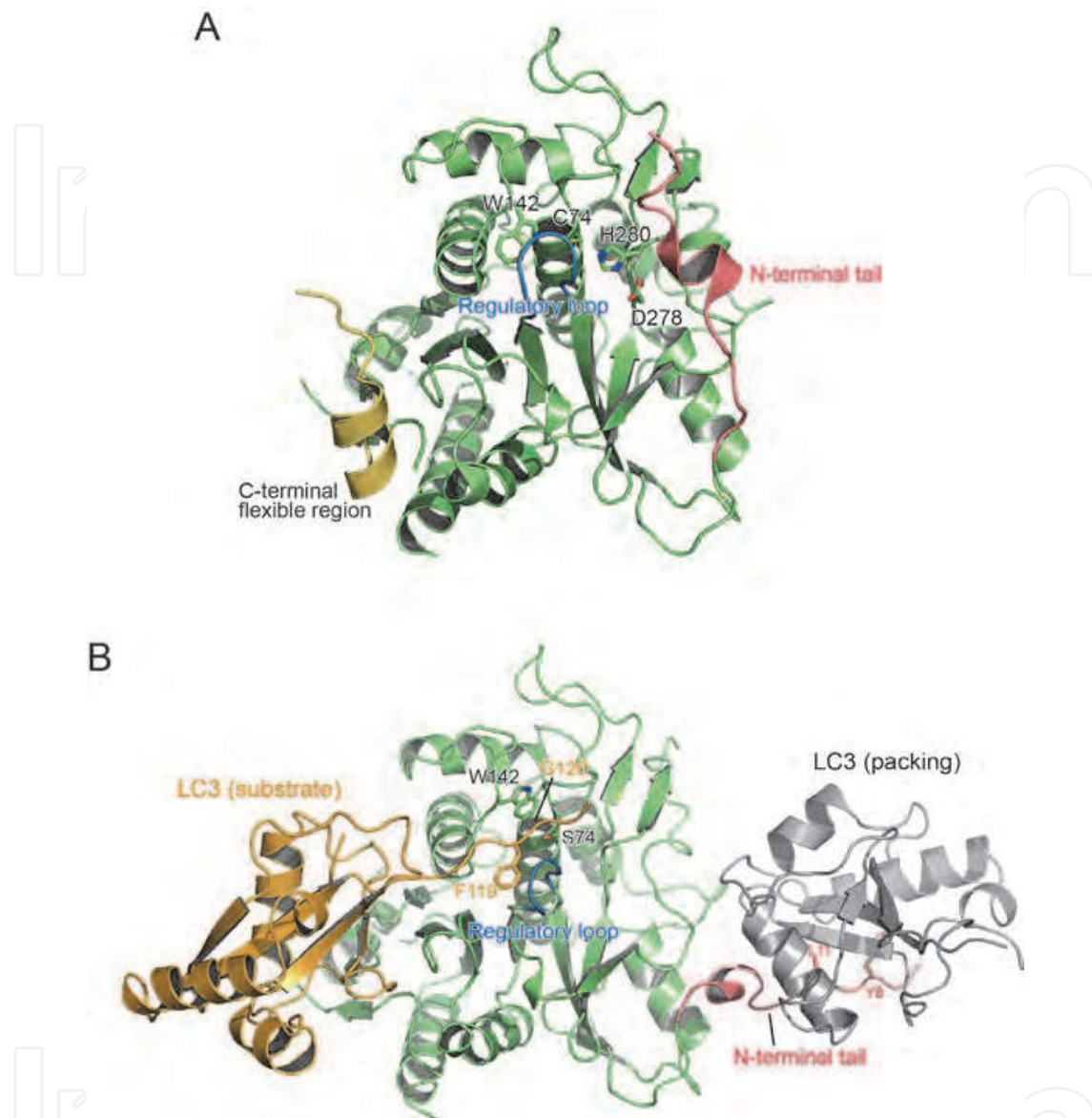


Fig. 5. Structure of HsAtg4B. (A) Free HsAtg4B structure. N-terminal region, regulatory loop as well as C-terminal flexible region are colored salmon pink, blue and yellow, respectively. (B). HsAtg4B-LC3 precursor complex structure. LC3 bound to the catalytic site of HsAtg4B is colored light orange, while LC3 bound to the N-terminal tail of HsAtg4B is colored gray. The other coloring is as in (A).

We obtained two HsAtg4B-LC3 precursor complex structures: one has a C74S mutation and the other has an H280A mutation in HsAtg4B. Each mutation completely abolishes the activity of HsAtg4B, and the LC3 precursor in both crystals actually remains intact. However, the two mutations have different effects on the conformation of the catalytic site: the H280A mutation affects the conformation of Cys74 and the bound C-terminal tail of LC3, whereas the C74S mutation does not. Thus, it is important for us to select an appropriate mutant for the structural study of the enzyme-substrate complex.

## 2.5 Atg5-Atg16 complex

Atg5 is the sole target for Atg12 modification. The side-chain of Atg5 Lys149 forms an isopeptide bond with Atg12 Gly186. Atg5 also interacts with Atg16 non-covalently, on which Atg12 conjugation has no effect. In yeast, Atg5 is presumed to function only as the Atg12–Atg5-Atg16 complex. The Atg12–Atg5-Atg16 complex localizes to isolation membranes and play crucial roles in autophagosome formation. Using an *in vitro* reconstitution system, we showed that the Atg12–Atg5 conjugate functions as an E3-like enzyme and accelerates the conjugation reaction between Atg8 and PE (Fujioka et al., 2008a; Hanada et al., 2007). We showed that Atg12 has a ubiquitin-like structure (see above); however, Atg5 and Atg16 have little sequential homology not only with known E3 enzymes but also with protein whose structure has already been reported. Therefore, in order to elucidate the overall architecture of the Atg12–Atg5-Atg16 complex, we started structural studies on Atg5 and Atg16.

### 2.5.1 Atg5 complexed with the N-terminal region of Atg16

*S. cerevisiae* Atg5 and Atg16 consist of 294 and 150 amino acids, respectively. We first attempted to crystallize full-length Atg5 alone, but failed owing to the low expression level of Atg5 in *E. coli* and its aggregate-prone nature. It was reported that Atg5 forms a stable complex with Atg16 *in vivo*. Therefore, we considered that Atg5 can be stabilized in *E. coli* by coexpression with Atg16. In fact, coexpression of Atg16 markedly increased the expression level of Atg5, thereby improving the solubility of Atg5. We then succeeded in obtaining a stable Atg5-Atg16 complex. It behaved as a complex throughout the entire purification process, suggesting that the affinity between them is significantly high. Using the purified complex, we started crystallization trials. However, the full-length Atg5-Atg16 complex did not crystallize at all. Atg16 alone was easily cleaved at the C-terminal side of Phe46 by contaminated proteases, and the N-terminal portion of the cleaved sample (residues 1-46) also formed a stable complex with Atg5. Therefore, we next used the Atg5-Atg16(1-46) complex for crystallization, and succeeded in obtaining good crystals (Matsushita et al., 2006). The crystal structure of the Atg5-Atg16(1-46) complex was determined by MIR in combination with MAD (Matsushita et al., 2007). We also attempted to crystallize the Atg5-Atg16 complex with Atg16 of various lengths. We obtained the Atg5-Atg16(1-57) complex crystal, but failed to obtain complex crystals containing Atg16 longer than 57 amino acids. The crystal structure of the Atg5-Atg16(1-57) complex was determined by the molecular replacement method.

The two complex structures are essentially identical with each other except for the non-overlapping region (residues 47-57 of Atg16). Atg5 has a unique structure consisting of two ubiquitin-like domains and a helix-rich domain between them (Figure 6A). These three domains interact with each other to form a globular fold. Lys149, the conjugation site for Atg12, is located at the helix-rich domain and has an exposed side chain. The N-terminal region of Atg16 is composed of an  $\alpha$ -helix (residues 22-40) and its downstream loop (residues 41-57). The  $\alpha$ -helix moiety binds to the groove formed by the three domains of Atg5, while the loop region binds to the N-terminal ubiquitin-like domain. These two structures and results of a mutational analysis suggested that residues 22-46 of Atg16 are the minimum region required for Atg5 binding. Lys149 and the residues involved in Atg16 binding are located distally to each other, which is consistent with the observation that the conjugation of Atg12 to Atg5 does not affect the Atg5-Atg16 interaction.

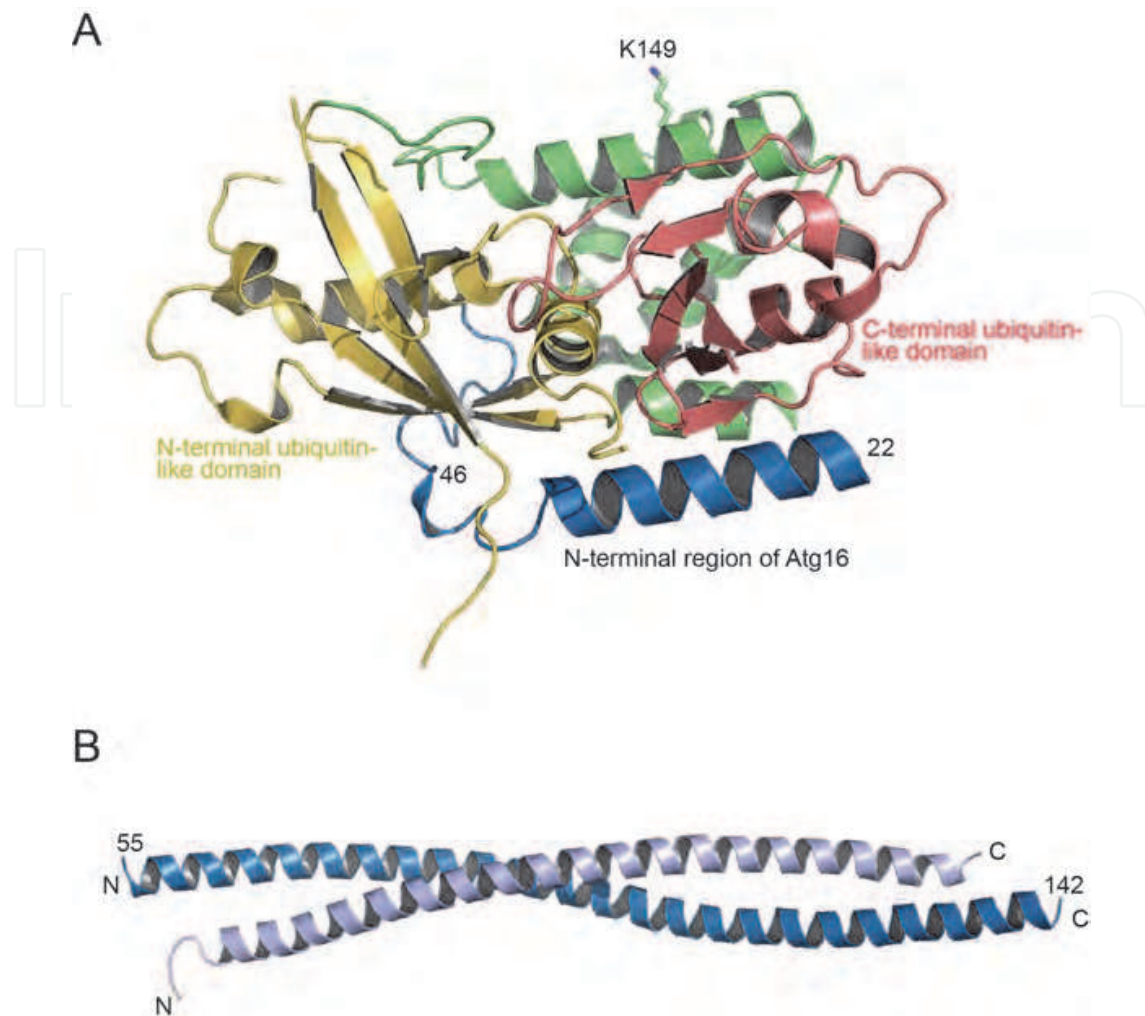


Fig. 6. Structure of Atg5 and Atg16. (A) Structure of Atg5 complexed with the N-terminal region (residues 1-57) of Atg16. N- and C-terminal ubiquitin-like domains and the other region are colored yellow, salmon pink and green, respectively, while N-terminal region of Atg16 is colored blue. (B) Structure of the coiled-coil dimer of full-length Atg16. One molecule is colored blue, while the other is colored light blue. N- and C-termini are labeled N and C, respectively.

### 2.5.2 Atg16

Although the structure of the N-terminal Atg5-binding region of Atg16 was determined as a complex with Atg5, that of the C-terminal region of Atg16 lacked structural information. From the primary sequence, the C-terminal region of Atg16 was predicted to contain a coiled-coil motif. Furthermore, on the basis of the results of gel-filtration chromatography experiments, Atg16 was suggested to form a multimer, possibly a tetramer, through the coiled-coil motif (Kuma et al., 2002). In order to determine the overall architecture of Atg16, we performed crystallization trials on Atg16 constructs of various lengths containing the predicted coiled-coil motif. Most of the tested constructs crystallized; however, these crystals diffracted poorly (6~8 Å resolution), except for one corresponding to residues 50-123 of Atg16 (Fujioka et al., 2008b). Since Atg16(50-123) does not have a Met residue, Leu103 was replaced with Met and using this construct, selenomethionine-labeled crystals were

prepared and used for single anomalous dispersion (SAD) phasing. The crystal structure of Atg16(50-123) is composed of one  $\alpha$ -helix of 90 Å length (Fujioka et al., 2010). The asymmetric unit contains six Atg16(50-123) molecules, which form three similar parallel coiled-coil dimers. These coiled-coil dimers expose two acidic residues (Asp101 and Glu102). By replacing these acidic residues with alanine, we succeeded in obtaining good crystals of full-length Atg16 and determined the structure by the molecular replacement method (Fujioka et al., 2010). The crystal structure of full-length Atg16 (D101A+E102A) is composed of one  $\alpha$ -helix of 130 Å length. The structure lacked the electron density of the N-terminal region (residues 1-54), suggesting that the N-terminal region has various orientations relative to the C-terminal region. The asymmetric unit contained two Atg16 molecules, which formed a parallel coiled-coil dimer similar to the Atg16(50-123) dimer (Figure 6B). In both crystals, various interactions were observed between the coiled-coil dimers. In order to establish the oligomerization state of Atg16 in solution, we performed analytical ultracentrifugation experiments, which showed that Atg16 exists as a homodimer in solution (Fujioka et al., 2010) and that the Atg5-Atg16 complex exists as a 2:2 heterotetramer in solution. These data are consistent with the coiled-coil dimer structure of Atg16 observed in both crystals, suggesting that Atg16 forms a dimer but not a tetramer in solution.

The obtained structural and biochemical information suggested that the overall architecture of the Atg5-Atg16 complex is composed of two sets of the N-terminal short  $\alpha$ -helix of Atg16 bound to Atg5, the C-terminal parallel coiled-coil homodimer of Atg16, and flexible linkers connecting them, resulting in a 2:2 complex. Since Atg12 is conjugated to Lys149 of each Atg5, the Atg12-Atg5-Atg16 complex forms a 2:2:2 complex. The overall architecture of the Atg12-Atg5-Atg16 complex, which is quite unique compared with any structure-reported proteins including other E3 enzymes, will be one basis for studying the molecular functions of this unique protein complex in autophagy.

### 3. Conclusion

Obtaining good crystals is the rate-limiting step of X-ray crystallography. We have no versatile method for obtaining good crystals and thus have attempted the crystallization of each protein through trial and error. However, accumulated experience will increase the probability of obtaining good crystals and accelerate structural studies. We started a comprehensive structural study of Atg proteins about ten years ago, and have already obtained good crystals for more than ten Atg proteins that include not only those involved in conjugation reactions but also those involved in the construction of the pre-autophagosomal structure (Suzuki and Ohsumi, 2010). Continuous trials will surely provide us with good crystals for all the Atg proteins, and through the comprehensive structural study of these protein crystals, the molecular mechanism of autophagy will be established in the near future.

### 4. Acknowledgment

This work was supported by Grants-in-Aid for Scientific Research on Priority Areas and Targeted Proteins Research Program from the Ministry of Education, Culture, Sports, Science and Technology of Japan.

## 5. References

- Fujioka, Y., Noda, N.N., Fujii, K., Yoshimoto, K., Ohsumi, Y. & Inagaki, F. (2008a). In vitro reconstitution of plant Atg8 and Atg12 conjugation systems essential for autophagy. *J Biol Chem*, Vol.283, No.4, Jan 25, pp. 1921-1928, 0021-9258
- Fujioka, Y., Noda, N.N., Matsushita, M., Ohsumi, Y. & Inagaki, F. (2008b). Crystallization of the coiled-coil domain of Atg16 essential for autophagy. *Acta Crystallogr Sect F Struct Biol Cryst Commun*, Vol.64, No.Pt 11, Nov 1, pp. 1046-1048, 1744-3091
- Fujioka, Y., Noda, N.N., Nakatogawa, H., Ohsumi, Y. & Inagaki, F. (2010). Dimeric coiled-coil structure of *Saccharomyces cerevisiae* Atg16 and its functional significance in autophagy. *J Biol Chem*, Vol.285, No.2, Jan 8, pp. 1508-1515, 0021-9258
- Hanada, T., Noda, N.N., Satomi, Y., Ichimura, Y., Fujioka, Y., Takao, T., Inagaki, F. & Ohsumi, Y. (2007). The Atg12-Atg5 conjugate has a novel E3-like activity for protein lipidation in autophagy. *J Biol Chem*, Vol.282, No.52, Dec 28, pp. 37298-37302, 0021-9258
- Hanada, T. & Ohsumi, Y. (2005). Structure-function relationship of Atg12, a ubiquitin-like modifier essential for autophagy. *Autophagy*, Vol.1, No.2, Jul, pp. 110-118, 1554-8627
- Ichimura, Y., Kirisako, T., Takao, T., Satomi, Y., Shimonishi, Y., Ishihara, N., Mizushima, N., Tanida, I., Kominami, E., Ohsumi, M., *et al.* (2000). A ubiquitin-like system mediates protein lipidation. *Nature*, Vol.408, No.6811, Nov 23, pp. 488-492, 0028-0836
- Kabeya, Y., Mizushima, N., Ueno, T., Yamamoto, A., Kirisako, T., Noda, T., Kominami, E., Ohsumi, Y. & Yoshimori, T. (2000). LC3, a mammalian homologue of yeast Apg8p, is localized in autophagosome membranes after processing. *EMBO J*, Vol.19, No.21, Nov 1, pp. 5720-5728, 0261-4189
- Kabeya, Y., Mizushima, N., Yamamoto, A., Oshitani-Okamoto, S., Ohsumi, Y. & Yoshimori, T. (2004). LC3, GABARAP and GATE16 localize to autophagosomal membrane depending on form-II formation. *J Cell Sci*, Vol.117, No.Pt 13, Jun 1, pp. 2805-2812, 0021-9533
- Kirisako, T., Baba, M., Ishihara, N., Miyazawa, K., Ohsumi, M., Yoshimori, T., Noda, T. & Ohsumi, Y. (1999). Formation process of autophagosome is traced with Apg8/Aut7p in yeast. *J Cell Biol*, Vol.147, No.2, Oct 18, pp. 435-446, 0021-9525
- Kirisako, T., Ichimura, Y., Okada, H., Kabeya, Y., Mizushima, N., Yoshimori, T., Ohsumi, M., Takao, T., Noda, T. & Ohsumi, Y. (2000). The reversible modification regulates the membrane-binding state of Apg8/Aut7 essential for autophagy and the cytoplasm to vacuole targeting pathway. *J Cell Biol*, Vol.151, No.2, Oct 16, pp. 263-276, 0021-9525
- Klionsky, D.J., Cregg, J.M., Dunn, W.A., Jr., Emr, S.D., Sakai, Y., Sandoval, I.V., Sibirny, A., Subramani, S., Thumm, M., Veenhuis, M., *et al.* (2003). A unified nomenclature for yeast autophagy-related genes. *Dev Cell*, Vol.5, No.4, Oct, pp. 539-545, 1534-5807
- Kuma, A., Mizushima, N., Ishihara, N. & Ohsumi, Y. (2002). Formation of the approximately 350-kDa Apg12-Apg5-Apg16 multimeric complex, mediated by Apg16 oligomerization, is essential for autophagy in yeast. *J Biol Chem*, Vol.277, No.21, May 24, pp. 18619-18625, 0021-9258
- Kumeta, H., Watanabe, M., Nakatogawa, H., Yamaguchi, M., Ogura, K., Adachi, W., Fujioka, Y., Noda, N.N., Ohsumi, Y. & Inagaki, F. (2010). The NMR structure of the autophagy-related protein Atg8. *J Biomol NMR*, Vol.47, No.3, Jul, pp. 237-241, 1573-5001

- Matsushita, M., Suzuki, N.N., Fujioka, Y., Ohsumi, Y. & Inagaki, F. (2006). Expression, purification and crystallization of the Atg5-Atg16 complex essential for autophagy. *Acta Crystallogr Sect F Struct Biol Cryst Commun*, Vol.62, Pt 10, Oct 1, pp. 1021-1023, 1744-3091
- Matsushita, M., Suzuki, N.N., Obara, K., Fujioka, Y., Ohsumi, Y. & Inagaki, F. (2007). Structure of Atg5-Atg16, a complex essential for autophagy. *J Biol Chem*, Vol.282, No.9, Mar 2, pp. 6763-6772, 0021-9258
- Mizushima, N. (2007). Autophagy: process and function. *Genes Dev*, Vol.21, No.22, Nov 15, pp. 2861-2873, 0890-9369
- Mizushima, N., Kuma, A., Kobayashi, Y., Yamamoto, A., Matsubae, M., Takao, T., Natsume, T., Ohsumi, Y. & Yoshimori, T. (2003). Mouse Apg16L, a novel WD-repeat protein, targets to the autophagic isolation membrane with the Apg12-Apg5 conjugate. *J Cell Sci*, Vol.116, No.Pt 9, May 1, pp. 1679-1688, 0021-9533
- Mizushima, N., Levine, B., Cuervo, A.M. & Klionsky, D.J. (2008). Autophagy fights disease through cellular self-digestion. *Nature*, Vol.451, No.7182, Feb 28, pp. 1069-1075, 1476-4687
- Mizushima, N., Noda, T. & Ohsumi, Y. (1999). Apg16p is required for the function of the Apg12p-Apg5p conjugate in the yeast autophagy pathway. *EMBO J*, Vol.18, No.14, Jul 15, pp. 3888-3896, 0261-4189
- Mizushima, N., Noda, T., Yoshimori, T., Tanaka, Y., Ishii, T., George, M.D., Klionsky, D.J., Ohsumi, M. & Ohsumi, Y. (1998). A protein conjugation system essential for autophagy. *Nature*, Vol.395, No.6700, Sep 24, pp. 395-398, 0028-0836
- Mizushima, N., Yoshimori, T. & Levine, B. (2010). Methods in mammalian autophagy research. *Cell*, Vol.140, No.3, Feb 5, pp. 313-326, 1097-4172
- Mizushima, N., Yoshimori, T. & Ohsumi, Y. (2011). The Role of Atg Proteins in Autophagosome Formation. *Annu Rev Cell Dev Biol*, Vol.27, Nov 10, pp. 107-132, 1530-8995
- Nakatogawa, H., Ichimura, Y. & Ohsumi, Y. (2007). Atg8, a ubiquitin-like protein required for autophagosome formation, mediates membrane tethering and hemifusion. *Cell*, Vol.130, No.1, Jul 13, pp. 165-178, 0092-8674
- Nakatogawa, H., Suzuki, K., Kamada, Y. & Ohsumi, Y. (2009). Dynamics and diversity in autophagy mechanisms: lessons from yeast. *Nat Rev Mol Cell Biol*, Vol.10, No.7, Jul, pp. 458-467, 1471-0080
- Noda, N.N., Fujioka, Y., Ohsumi, Y. & Inagaki, F. (2008a). Crystallization of the Atg12-Atg5 conjugate bound to Atg16 by the free-interface diffusion method. *Journal of synchrotron radiation*, Vol.15, No.Pt 3, May, pp. 266-268, 0909-0495
- Noda, N.N., Kumeta, H., Nakatogawa, H., Satoo, K., Adachi, W., Ishii, J., Fujioka, Y., Ohsumi, Y. & Inagaki, F. (2008b). Structural basis of target recognition by Atg8/LC3 during selective autophagy. *Genes Cells*, Vol.13, No.12, Dec, pp. 1211-1218, 1365-2443
- Noda, N.N., Ohsumi, Y. & Inagaki, F. (2009). ATG systems from the protein structural point of view. *Chem Rev*, Vol.109, No.4, Apr, pp. 1587-1598, 1520-6890
- Noda, N.N., Ohsumi, Y. & Inagaki, F. (2010). Atg8-family interacting motif crucial for selective autophagy. *FEBS Lett*, Vol.584, No.7, Apr 2, pp. 1379-1385, 1873-3468

- Radoshevich, L., Murrow, L., Chen, N., Fernandez, E., Roy, S., Fung, C. & Debnath, J. (2010). ATG12 conjugation to ATG3 regulates mitochondrial homeostasis and cell death. *Cell*, Vol.142, No.4, Aug 20, pp. 590-600, 1097-4172
- Satoo, K., Noda, N.N., Kumeta, H., Fujioka, Y., Mizushima, N., Ohsumi, Y. & Inagaki, F. (2009). The structure of Atg4B-LC3 complex reveals the mechanism of LC3 processing and delipidation during autophagy. *EMBO J*, Vol.28, No.9, May 6, pp. 1341-1350, 1460-2075
- Satoo, K., Suzuki, N.N., Fujioka, Y., Mizushima, N., Ohsumi, Y. & Inagaki, F. (2007). Crystallization and preliminary crystallographic analysis of human Atg4B-LC3 complex. *Acta Crystallogr Sect F Struct Biol Cryst Commun*, Vol.63, No.Pt 2, Feb 1, pp. 99-102, 1744-3091
- Scott, S.V., Guan, J., Hutchins, M.U., Kim, J. & Klionsky, D.J. (2001). Cvt19 is a receptor for the cytoplasm-to-vacuole targeting pathway. *Mol Cell*, Vol.7, No.6, Jun, pp. 1131-1141, 1097-2765
- Shintani, T., Mizushima, N., Ogawa, Y., Matsuura, A., Noda, T. & Ohsumi, Y. (1999). Apg10p, a novel protein-conjugating enzyme essential for autophagy in yeast. *EMBO J*, Vol.18, No.19, Oct 1, pp. 5234-5241, 0261-4189
- Sugawara, K., Suzuki, N.N., Fujioka, Y., Mizushima, N., Ohsumi, Y. & Inagaki, F. (2003). Crystallization and preliminary X-ray analysis of LC3-I. *Acta Crystallogr D Biol Crystallogr*, Vol.59, No.Pt 8, Aug, pp. 1464-1465, 0907-4449
- Sugawara, K., Suzuki, N.N., Fujioka, Y., Mizushima, N., Ohsumi, Y. & Inagaki, F. (2004). The crystal structure of microtubule-associated protein light chain 3, a mammalian homologue of *Saccharomyces cerevisiae* Atg8. *Genes Cells*, Vol.9, No.7, Jul, pp. 611-618, 1356-9597
- Sugawara, K., Suzuki, N.N., Fujioka, Y., Mizushima, N., Ohsumi, Y. & Inagaki, F. (2005). Structural basis for the specificity and catalysis of human Atg4B responsible for mammalian autophagy. *J Biol Chem*, Vol.280, No.48, Dec 2, pp. 40058-40065, 0021-9258
- Suzuki, N.N., Yoshimoto, K., Fujioka, Y., Ohsumi, Y. & Inagaki, F. (2005). The crystal structure of plant ATG12 and its biological implication in autophagy. *Autophagy*, Vol.1, No.2, Jul, pp. 119-126, 1554-8627
- Suzuki, K. & Ohsumi, Y. (2010). Current knowledge of the pre-autophagosomal structure (PAS). *FEBS Lett*, Vol.584, No.7, Apr 2, pp. 1280-1286, 1873-3468
- Tanida, I., Mizushima, N., Kiyooka, M., Ohsumi, M., Ueno, T., Ohsumi, Y. & Kominami, E. (1999). Apg7p/Cvt2p: A novel protein-activating enzyme essential for autophagy. *Mol Biol Cell*, Vol.10, No.5, May, pp. 1367-1379, 1059-1524
- Tsukada, M. & Ohsumi, Y. (1993). Isolation and characterization of autophagy-defective mutants of *Saccharomyces cerevisiae*. *FEBS Lett*, Vol.333, No.1-2, Oct 25, pp. 169-174, 0014-5793
- Yamada, Y., Suzuki, N.N., Fujioka, Y., Ichimura, Y., Ohsumi, Y. & Inagaki, F. (2006). Crystallization and preliminary X-ray analysis of Atg3. *Acta Crystallographica Section F: Structural Biology and Crystallization Communication*, Vol.62, Pt 10, Oct 1, pp. 1016-1017, 1744-3091
- Yamada, Y., Suzuki, N.N., Hanada, T., Ichimura, Y., Kumeta, H., Fujioka, Y., Ohsumi, Y. & Inagaki, F. (2007). The crystal structure of Atg3, an autophagy-related ubiquitin

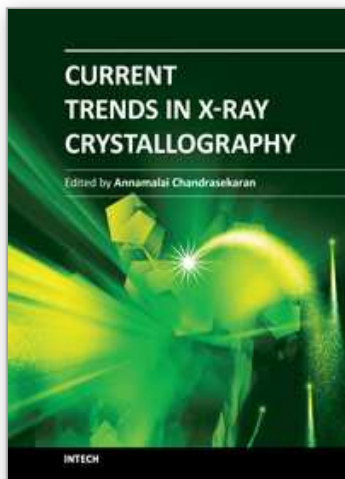


carrier protein (E2) enzyme that mediates Atg8 lipidation. *J Biol Chem*, Vol.282, No.11, Mar 16, pp. 8036-8043, 0021-9258

Yamaguchi, M., Noda, N.N., Nakatogawa, H., Kumeta, H., Ohsumi, Y. & Inagaki, F. (2010). Autophagy-related protein 8 (Atg8) family interacting motif in Atg3 mediates the Atg3-Atg8 interaction and is crucial for the cytoplasm-to-vacuole targeting pathway. *J Biol Chem*, Vol.285, No.38, Sep 17, pp. 29599-29607, 0021-9258

IntechOpen

IntechOpen



## **Current Trends in X-Ray Crystallography**

Edited by Dr. Annamalai Chandrasekaran

ISBN 978-953-307-754-3

Hard cover, 436 pages

**Publisher** InTech

**Published online** 16, December, 2011

**Published in print edition** December, 2011

This book on X-ray Crystallography is a compilation of current trends in the use of X-ray crystallography and related structural determination methods in various fields. The methods covered here include single crystal small-molecule X-ray crystallography, macromolecular (protein) single crystal X-ray crystallography, and scattering and spectroscopic complimentary methods. The fields range from simple organic compounds, metal complexes to proteins, and also cover the meta-analyses of the database for weak interactions.

### **How to reference**

In order to correctly reference this scholarly work, feel free to copy and paste the following:

Nobuo N. Noda, Yoshinori Ohsumi and Fuyuhiko Inagaki (2011). Crystallographic Studies on Autophagy-Related Proteins, Current Trends in X-Ray Crystallography, Dr. Annamalai Chandrasekaran (Ed.), ISBN: 978-953-307-754-3, InTech, Available from: <http://www.intechopen.com/books/current-trends-in-x-ray-crystallography/crystallographic-studies-on-autophagy-related-proteins>

**INTECH**  
open science | open minds

### **InTech Europe**

University Campus STeP Ri  
Slavka Krautzeka 83/A  
51000 Rijeka, Croatia  
Phone: +385 (51) 770 447  
Fax: +385 (51) 686 166  
[www.intechopen.com](http://www.intechopen.com)

### **InTech China**

Unit 405, Office Block, Hotel Equatorial Shanghai  
No.65, Yan An Road (West), Shanghai, 200040, China  
中国上海市延安西路65号上海国际贵都大饭店办公楼405单元  
Phone: +86-21-62489820  
Fax: +86-21-62489821

© 2011 The Author(s). Licensee IntechOpen. This is an open access article distributed under the terms of the [Creative Commons Attribution 3.0 License](#), which permits unrestricted use, distribution, and reproduction in any medium, provided the original work is properly cited.

IntechOpen

IntechOpen